The Journal of Experimental Biology 210, 815-824
Published by The Company of Biologists 2007
doi:10.1242/jeb.001867

Morphometry of retinal vasculature in Antarctic fishes is dependent upon the level of hemoglobin in circulation

Jody M. Wujcik[1], George Wang[2], Joseph T. Eastman[3] and Bruce D. Sidell[1,*]

[1]*School of Marine Sciences, University of Maine, 5751 Murray Hall, Orono, ME 04469-5751, USA,* [2]*Department of Biology, University of Washington, Box 351800, Seattle, WA 98195-1800, USA and* [3]*Department of Biomedical Sciences, Ohio University, Athens, OH 45701-2979, USA*

*Author for correspondence (e-mail: bsidell@maine.edu)

Accepted 3 January 2007

Summary

We quantitatively assessed ocular vascular patterns of six Antarctic notothenioid fishes that vary in their expression of the circulating oxygen-binding protein, hemoglobin (Hb). Digital image analyses revealed marked differences in vessel morphometries among notothenioid species. Hemoglobinless (–Hb) icefishes display mean vessel length densities that are greater (*Chaenocephalus aceratus*, 5.51±0.32 mm mm^{-2}; *Champsocephalus gunnari*, 5.15±0.50 mm mm^{-2}) than those observed in red-blooded (+Hb) species (*Gymnodraco acuticeps*, 5.20±0.46 mm mm^{-2}; *Parachaenichthyes charcoti*, 4.40±0.30 mm mm^{-2}; *Trematomus hansoni*, 3.94±0.08 mm mm^{-2}; *Notothenia coriiceps*, 2.48±0.21 mm mm^{-2}). –Hb fishes also have mean vessel diameters that are ~1.5 times greater than vessel diameters of +Hb species (–Hb, 0.193±0.006 mm; +Hb, 0.125±0.005 mm). Vascular density index (VDI), a stereological index that is affected by both vessel number and length, is greatest in –Hb *C. aceratus* (3.51±0.20) and lowest in +Hb *N. coriiceps* (1.58±0.14). Among four +Hb species, there is a direct relationship between red blood cell content and retinal vasculature. Hematocrit (Hct) is inversely correlated to vascular density (r^2=0.934) and positively correlated to intervessel distance (r^2= 0.898) over a >2.3-fold range of Hct. These results indicate that anatomical capacity to supply blood to the retina increases to compensate for decreases in oxygen-carrying capacity of the blood.

Key words: Antarctic fish, hemoglobin, retina, vascular density, icefish, notothenioid, hematocrit, nitric oxide, circulation, morphometry.

Introduction

The Southern Ocean encompasses over 35×10^6 km^2, approximately 10% of the world's ocean (Laws, 1985). It is the coldest, densest, and most thermally stable marine habitat on the planet. Continental shelf waters continuously hover near or below 0°C and vary little seasonally or as a function of water depth (Knox, 1970; Lewis and Perkin, 1985). Although presenting a number of physiological challenges, cold temperatures do have a benefit. Because gaseous solubility is inversely proportional to temperature, oxygen content in Antarctic waters is extremely high. These conditions preclude marine organisms of the Southern Ocean from experiencing environmental hypoxia under normal circumstances (Littlepage, 1965).

Despite the harsh environmental conditions, one group of fishes has flourished in the Southern Ocean. Species of the perciform suborder Notothenioidei dominate the fish fauna of waters south of the Antarctic Polar Front. Notothenioids encompass 8 families, 44 genera, and 129 species and account for approximately 45% of fish species and 90% of fish biomass in the region (Eastman, 1993; Eastman, 2005). Notothenioids radiated to dominate this marine system from an ancestral stock that survived a dramatic crash in fish species diversity of the Southern Ocean that occurred sometime within the last ca. 30 million years. Modern notothenioids occupy a variety of habitat niches; some species are benthic or epibenthic, while others are pelagic, semipelagic or cryopelagic (Gon and Heemstra, 1990). Activity levels vary among species from sedentary to active.

Similar to all other vertebrate groups, seven of the eight families of fishes within the suborder Notothenioidei have blood with hemoglobin-containing circulating erythrocytes. Hematocrits characteristic of these red-blooded species overlap values typical of temperate zone fishes, although absolute hemoglobin concentrations are generally lower than those of temperate zone species because of lower mean corpuscular hemoglobin concentrations (Egginton, 1996). Among red-blooded notothenioid fishes, behavioral activities are correlated with concentrations of circulating hemoglobin (Hb) and number of erythrocytes, which are higher in more active species (Wells et al., 1980).

A single family of notothenioids, the channichthyid icefishes, are the only known vertebrate animals to lack Hb

completely as adults (Ruud, 1954). In the absence of Hb, oxygen is carried strictly in physical solution in icefish blood. This results in an oxygen-carrying capacity in icefishes that is <10% of that seen in closely related red-blooded species (Holeton, 1970). Modifications of the cardiovascular system of icefishes compensate for the complete absence of oxygen-binding Hb. Icefishes possess large-bore capillaries and have blood volumes that are 2–4 times larger than those of red-blooded fishes (Fitch et al., 1984; Hemmingsen and Douglas, 1970). Additionally, hearts are larger in icefishes than in similar-sized red-blooded fishes, resulting in mass-specific cardiac outputs that are several-fold greater than those of red-blooded species (Hemmingsen et al., 1972; Holeton, 1970). Integration of these features allows channichthyids to circulate large blood volumes at relatively high flow rates. This is achieved at low arterial blood pressures due to decreased systemic resistance to flow. Ultimately, the combination of high-throughput cardiovascular systems, waters of high oxygen content, and low absolute metabolic rates enables this group of fishes to deliver sufficient oxygen to their tissues (Hemmingsen, 1991).

Hemmingsen and Douglas (Hemmingsen and Douglas, 1970) first recognized that "*The large blood volume of C. aceratus may be a manifestation of an increased vascularization*." In retrospect, this conclusion is somewhat axiomatic, given that the additional blood volume must be accommodated somewhere within the vascular tree. Vasculature associated with the retina of the eye provides an excellent example and is exceptionally dense in Hb-lacking icefishes compared to Hb-expressing notothenioid species (Eastman, 1988; Eastman and Lannoo, 2004; Sidell and O'Brien, 2006). The vasculature of the teleost retina, especially in the case of channichthyids, differs in a number of respects from that of mammals and other fishes. Unlike mammals, most teleost retinae are avascular (Chase, 1982) and lack retinal arteries and veins within the substance of the retina. Furthermore, the retinae of fishes are generally thick, with diffusion distances as much as six times longer than in primates (Copeland, 1980). In order to satisfy the retinal requirement for oxygen, the teleostean eye has a dual blood supply from an ophthalmic artery derived from the pseudobranch and an optic artery from the internal carotid (Nicol, 1989). There are also three vascular structures not present in mammals: the choroid rete mirabile, the lentiform body (also a rete), and the falciform process (Walls, 1942; Nicol, 1989). Although present in phyletically basal notothenioids (Eastman and Lannoo, in press), channichthyids have lost the latter three structures and the ophthalmic artery may be vestigal or lost as well (Eastman and Lannoo, 2004). Thus the channichthyid retina is supplied by an optic artery that branches at the optic disk into an extensive series of hyaloid arteries at the vitreoretinal interface (Fig. 1A). These arteries are thin-walled (Eastman and Lannoo, 2004) and serve as large bore arterial capillaries. Veins do not accompany the hyaloid arteries in teleosts that have lost the ocular vascular structures mentioned above (Copeland, 1980; Nicol, 1989). This has been documented in histological studies of the retinae of various notothenioids (Eastman, 1988; Eastman and Lannoo, 2003), including channichthyids (Eastman and Lannoo, 2004). The hyaloid arteries drain to an annular vein located in the vicinity of the ora serrata at the retinal periphery (Fig. 3B).

Close spacing of hyaloid arteries in channichthyids effectively reduces the diffusion distance for oxygen, thus ensuring greater oxygenation of the underlying retina. This is highly beneficial to fishes that are already compromised by a reduction in oxygen-carrying capacity brought about by loss of Hb. From a practical standpoint, retinal vasculature is also a very attractive study system because the blood vessels are arrayed in an essentially two-dimensional pattern over the retinal tissue. As a consequence, they are much more tractable to visualization and quantification without necessitating three-dimensional reconstruction of tissue.

Retinae of notothenioid fishes are highly aerobically poised in metabolism (Waser and Heisler, 2004) and, like brain (Kawall et al., 2002), retinal oxygen demand should be relatively independent of locomotory activity level in these species. Given that oxygen-carrying capacity of blood can vary considerably, both among the red-blooded (+Hb) notothenioids and certainly between those families and the hemoglobinless (–Hb) icefishes, it seems reasonable to expect that anatomical and/or physiological compensations must ensure adequate oxygenation of the tissue among these fishes. The known physiological compensations of the cardiovascular system in –Hb species are relatively well characterized, as outlined above. To investigate possible anatomical compensations, we undertook the present study with objectives to: (1) quantify morphometric parameters of retinal vasculature in several species of both +Hb and –Hb Antarctic notothenioids and (2) assess the relationship between vascular patterns and hemoglobin content of blood. Our results show a profound correlation between vascular patterns and hemoglobin content and further suggest an underlying mechanism for regulating this relationship.

Materials and methods

Animals

Six species of notothenioid fishes were collected from aboard the ARSV *Laurence M. Gould* in the austral autumn (April–May) of 2005 from waters of the Antarctic Peninsula region. *Chaenocephalus aceratus* (Lönnberg 1906), *Champsocephalus gunnari* Lönnberg 1905, *Gymnodraco acuticeps* Boulenger 1902, *Parachaenichthyes charcoti* (Vaillant 1906), and *Notothenia coriiceps* Richardson 1844 were primarily caught by otter trawl at 85–200 m depth near Astrolabe Needle (64°08′S, 62°40′W) in Dallman Bay. *Trematomus hansoni* Boulenger 1902 was captured in baited benthic pot traps at 250–500 m depth from either the Neumayer Channel (64°30′S, 62°34′W) or Palmer Basin (64°50′S, 64°04′W). Animals were kept in circulating seawater tanks and transported to the US Antarctic Palmer Station on Anvers Island, where they were maintained unfed, in covered aquaria

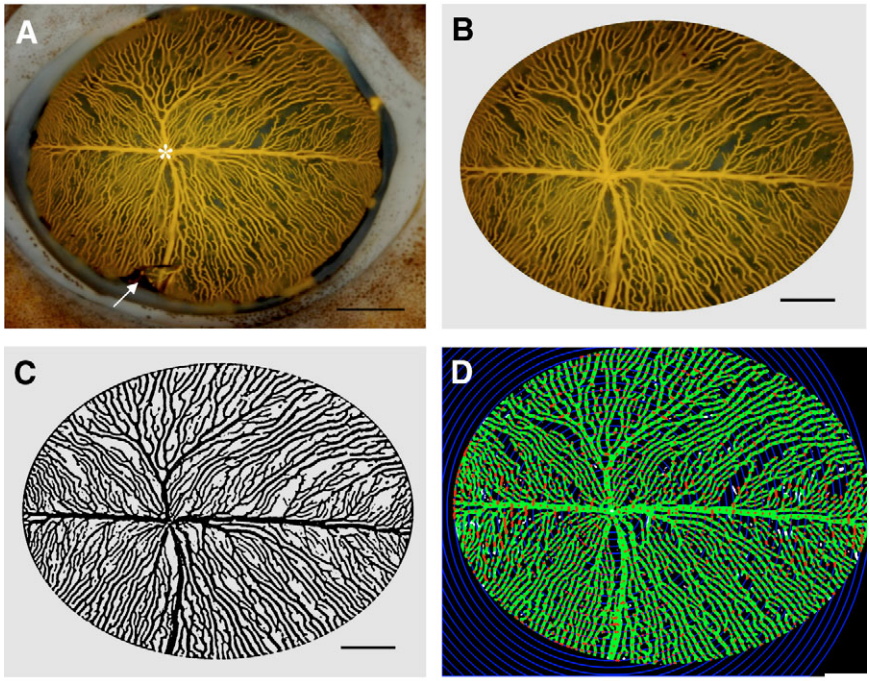

Fig. 1. Representative digital images of the hyaloid arteries on the vitrad surface of the retina of *Champsocephalus gunnari*, a white-blooded channichthyid. (A) Original digital image; (B) cropped image; (C) binary image; (D) binary image with superimposed concentric circle overlay. Grid spacing between successive circles is fixed at 0.5 mm and red markings indicate vessel–grid intersections. The asterisk denotes the optic disc and the arrow indicates the retractor lentis muscle in image A. Scale bars, 3 mm (A); 2 mm (B–D).

containing circulating seawater at –0.8±0.3°C.

Tissue preparation

To visualize vascular features, blood vessels of fishes were filled with Microfil^{TM} (Flow Tech, Inc., Carver, MA, USA), a liquid silicon rubber compound. Animals were first anesthetized with MS-222 in seawater (1:7500 w/v; 3-aminobenzoic acid ethyl ester; Sigma-Aldrich, St Louis, MO, USA) for a period of 10–15 min. After initial anesthetization, a blood sample (approximately 1 ml) was taken by caudal venipuncture from each red-blooded individual for determination of hematocrit (Hct). Next, concentrated heparinized notothenioid Ringer solution (2500 U ml^{-1} heparin added to 260 mmol l^{-1} NaCl, 2.5 mmol l^{-1} $MgCl_2{\cdot}6H_2O$, 5.0 mmol l^{-1} KCl, 2.5 mmol l^{-1} $NaHCO_3$, 5.0 mmol l^{-1} $NaH_2PO_4{\cdot}H_2O$, pH 8.0) was injected into the caudal vein at a dose of ~2.5 ml kg^{-1} and the animal was promptly returned to a holding tank for an additional 10 min. Fishes were then placed ventral side up on an iced surgical platform and a series of incisions were made to open the pericardial cavity. The atrium and ventricle were removed, leaving the bulbus arteriosus intact *in situ*. The bulbus arteriosus was cannulated with PE-tubing (90, 100, 160 or 190) and ligated with surgical silk. The cannula was then connected to tubing leading to a syringe loaded in a Model 100 syringe pump (KD Scientific Inc., Holliston, MA, USA). Approximately 15–30 ml of ice-cold heparinized notothenioid Ringer solution (760 U ml^{-1} heparin added to 260 mmol l^{-1} NaCl, 2.5 mmol l^{-1} $MgCl_2{\cdot}6H_2O$, 5.0 mmol l^{-1} KCl, 2.5 mmol l^{-1} $NaHCO_3$, 5.0 mmol l^{-1} $NaH_2PO_4{\cdot}H_2O$, pH 8.0) was perfused throughout the entire vascular system at a flow rate of ⩽46.8 ml h^{-1}. Specimens were then filled with 9–27 ml of ice-cold yellow Microfil^{TM} using the same apparatus at a flow rate of ⩽34.2 ml h^{-1} until venous return of the compound to the pericardial cavity was observed. While allowing the Microfil^{TM} to polymerize, specimens were maintained on ice for about 1 h, followed by a 1-week fixation in 10% formalin and subsequent storage in 70% ethanol.

Fixed specimens were transported back to our home laboratory at the University of Maine where eyes were excised from each specimen as part of an intact, rectangular block of tissue, approximately 3.5 cm×5.0 cm in dimension. To visualize the hyaloid arteries at the vitreoretinal interface, the cornea, iris and lens were removed anterior to the margin of the ora serrata and the vitreous body was carefully extracted from the vitreous chamber.

Photography

Digital images were taken using a Nikon D70 camera (Nikon Inc., Melville, NY, USA) fitted with a 60 mm AF Micro Nikkor lens (Nikon Inc., Melville, NY, USA) and mounted on a stand approximately 27–28 cm above the plane of the vessels. Images were shot in aperture mode (F51) to compensate for the large depth of field of the eye. During the photographic procedure, eyes were secured in a shallow Petri dish and covered with 70% ethanol. Several photographs were taken of each eye and the best image of the series was chosen for further processing.

Image processing

Original digital images were processed using ImageJ (Version 1.32; NIH, Bethesda, MD, USA). Images were cropped by centering an oval region of interest tool (ROI) over the optic disc and extending the ROI outward until point of contact with the retractor lentis, forming a reference field containing the majority (>90%) of the hyaloid arteries present at the vitreoretinal interface (Fig. 1A,B). This procedure eliminated peripheral sections of the image, which would be most subject to distortion due to curvature, and also ensured that equivalent relative reference fields of eyes were sampled despite both intrapecific and interspecific differences in eye size. Next, an RGB color split was performed to isolate the yellow vessels. An edge finder, FJ Laplacian plugin with a derivative smoothing scale of 3, was used on the yellow channel image to maximize detection of the vessels from the

background. The yellow channel was inverted and contrast and brightness enhanced by histogram equalization. We removed the remaining image noise by subtracting the original blue channel values from this enhanced edge image, and again enhanced brightness and contrast through histogram equalization. The resultant image was then converted to binary *via* the threshold function (Fig. 1C). For a few of the images, there were discrete areas where vessels did not fill with Microfil™. These regions were cropped from the reference field. As a processing control, vessel diameters from the binary image were compared to vessel diameters of the original image. Differences between the two never exceeded 5%.

Procedure for inadequately filled specimens

A successful vascular fill was considered to be one where ⩾90% of the hyaloid arteries on the vitrad surface of the retina were filled with Microfil™. *T. hansoni* and *N. coriiceps* did not meet this criterion; therefore an alternative method was devised to demonstrate the ocular vasculature of these species. Tissues were grossly stained with a solution of 1 part of 1% aqueous aniline blue in 10 parts of saturated aqueous picric acid for ~1–2 min. After rinsing with distilled water, each eye was dissected further and returned to 70% ethanol. Blood vessels were then discernable and further removal of the vitreous body was possible without destruction of previously obscured vessels. For most of the specimens, staining and subsequent dissection had to be repeated several times before the tissue was satisfactory for photography.

Digital images of the stained eyes were taken as previously described. Using Adobe Photoshop (Version 7.0; Adobe Systems, Inc., San Jose, CA, USA) each image was converted to grayscale and contrast was adjusted to give maximal differentiation between the vessels and background. A transparent layer was superimposed on top of the grayscale image and blood vessels were traced using a digitizing tablet (DrawingBoard III; GTCO CalComp Inc., Columbia, MD, USA), while simultaneously verifying the actual vessels under a dissecting microscope. The brightness and contrast of the digitized drawing were adjusted so that the grayscale background layer disappeared (turned white) and the vessel layer (already black) remained, thus completing the conversion of the image to binary.

Image analysis

Morphometric measurements of retinal vascularity were obtained using an automated macro developed in Matlab and the Matlab Image Processing Toolbox (Matlab Version 7.1; Matlab Image Processing Toolbox Version 5.02; The Mathworks, Inc., Natick, MA, USA). The design of the macro was based on previous studies analyzing angiogenic response (Maas et al., 1999; Strick et al., 1991). A concentric circle overlay was superimposed on each computerized binary image with the first circle centered directly over the optic disc (Fig. 1D). The diameter of the innermost circle was 1.0 mm and spacing between successive circles was fixed at 0.5 mm. Vascular density index (VDI), a stereological index that is affected by both blood vessel length and number, was computed by dividing the number of vessel–grid intersections by the total circumference of circles within the reference field. VDI was first calculated for the entire reference field of the vitreoretinal interface. Each image was entered into Matlab twice and the average of the counts was recorded as the mean VDI for that specimen. The difference between the two counts was used to assess intra-observer variability. The reference field was then divided into four quadrants (QI-ventrotemporal, QII-dorsotemporal, QIII-dorsonasal, QIV-ventronasal), with the optic disc as the point of origin, to analyze VDI as a function of location within the fundus.

In addition to VDI, several other morphometric measurements were obtained using the Matlab macro. Individual vessel diameters, measured to the outside vessel wall, were recorded at each vessel–grid intersection, averaged together and reported as a mean for the entire eye. The intervessel distance (IVD) for each gridline was calculated by dividing the circumference of the circle by the number of intersecting vessels. Once again, calculations were averaged for the entire vitreoretinal interface and IVD was reported as a mean. Length density, the length of vessels per unit area, was derived using the principle of Buffon by multiplying VDI by $\pi/2$ (Weibel, 1979). Data were collected for one other morphometric parameter; ImageJ was used to measure fractional image area (FIA), the percent of reference field covered by blood vessels. FIAs were calculated for entire eyes and quadrants.

Statistical analyses

Comparisons among the six species for each morphometric measurement were performed in SigmaStat (Version 3.1; Systat Software, Inc., Point Richmond, CA, USA) using a one-way ANOVA with a *post-hoc* Student–Newman–Keuls test for multiple pairwise comparisons of the means. The alpha value was set at $P \leqslant 0.05$. Linear least-squares regression was used to analyze the relationship between Hcts and the following: vascular densities, intervessel distances, specimen total lengths and specimen body masses. Additionally, intra-observer variability associated with operation of the Matlab macro was assessed. Variability was calculated by dividing the standard deviation of the paired differences between replicates by the overall mean VDI.

Results

Content of circulating erythrocytes

Characteristic red blood cell content of the four red-blooded notothenioid species examined varied over an approximately 2.3-fold range, from Hcts of 16.1% in *G. acuticeps* to 37.5% in *N. coriiceps* (Table 1). Within any of the four red-blooded species, Hct showed no significant relationship to body size ($r^2<0.50$ for each species).

General vascular patterns and morphometries

The overall vascular pattern in retinas of the six species examined appears to be influenced by erythrocyte content of their blood. The greatest vascular densities and most complex

Table 1. *Hematocrits and physical characteristics of Antarctic notothenioid fishes*

	Channichthyidae		Bathydraconidae		Nototheniidae	
	C. aceratus (–Hb)	*C. gunnari* (–Hb)	*G. acuticeps* (+Hb)	*P. charcoti* (+Hb)	*T. hansoni* (+Hb)	*N. coriiceps* (+Hb)
Hematocrit (%)	ND	ND	16.1±6.0	26.1±2.7	24.4±6.4	37.5±1.1*
Body mass range (g)	175–931	397–477	154–241	66–491	186–583	437–719
Total length range (cm)	33–51	39–42	30–34	25–42	25–36	33–37

Hematocrit (Hct) values are means ± s.e.m.; *N*=2 for *G. acuticeps*; *N*=5 for *P. charcoti*; *N*=3 for *T. hansoni*; *N*=4 for *N. coriiceps*.
ND, not determined; species does not express hemoglobin.
* denotes that *N. coriiceps* has a significantly greater Hct than *G. acuticeps* ($P \leqslant 0.05$).

branching patterns are seen in hemoglobinless (–Hb) icefishes. *C. aceratus* and *C. gunnari* display branching patterns where four or five main arteries exit the optic disc and divide into an anastomosing array of closely spaced parallel channels on the fundus of the eye (Fig. 2A,B). Both bathydraconid species showed a radial branching pattern of hyaloid arteries with the vascular density of *G. acuticeps* greater than that of *P. charcoti*. The latter species shows a density of arteries that is clearly lower than those of icefishes (Fig. 3A,B). Further reductions in densities of radially arranged arteries in the retina are observed in the red-blooded notothenid species, *T. hansoni* and *N. coriiceps* (Fig. 4A,B). *N. coriiceps* shows the most sparsely distributed vascular array of any species examined.

There is a general trend for length densities of retinal blood vessels to increase with decreasing red blood cell content (Table 2). Likewise, mean vessel diameters of –Hb icefishes are ~1.5-fold greater than those of +Hb bathydraconid species (vessel diameters of notothenid species could not be estimated for technical reasons – see Materials and methods). The combination of these features, i.e. greatest length densities and vessel diameters, in icefishes results in significantly greater FIAs (percent of reference area covered by blood vessels) than seen in +Hb bathydraconids. In combination, these observations indicate that species of fish that lack Hb have larger blood vessel surface areas available for gas exchange and possess vascular capacities capable of accommodating larger blood volumes than +Hb fishes.

In all species examined, FIA also varies as a function of location on the fundus of the eye. Ventrotemporal and ventronasal regions of the eye generally display the greatest FIA, indicating maximal blood vessel surface area in the region of the eye ventral to the optic disc (data not shown).

How close is the relationship between hematocrit and vascularity?

Two anatomical characteristics of the vasculature are particularly closely related to capacity for supplying oxygen to tissue, vascular density index (VDI) and intervessel distance (IVD). As its name implies, VDI is a stereological index of vascularity within a given reference area. IVD is the average path length between neighboring vessels and is thus equal to 2× the shortest pathway for gaseous diffusion between vessels and underlying retinal tissue. Assuming relatively similar rates of perfusion, one might anticipate that reductions in oxygen-carrying capacity of blood might be met with compensatory increases in VDI and decreases in IVD. To test this, we examined the correlation of Hct with each of these parameters within the red-blooded notothenioids examined in this study.

VDI shows a striking inverse correlation with Hct among the red-blooded species (r^2=0.934; red symbols in Fig. 5A). Not surprisingly, hemoglobinless species that have the lowest blood oxygen-carrying capacity of any of the fishes studied also show the densest vasculature (Table 2). Because the hemoglobinless icefishes are known to have substantially higher cardiac outputs than their red-blooded relatives, however, they are apparently able to adequately oxygenate their retinal tissue at a lower vascular density than would be predicted by the relationship among the

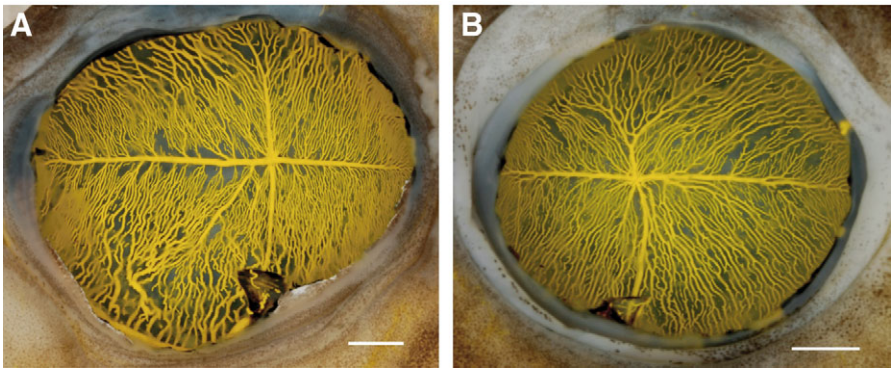

Fig. 2. Representative digital images of the hyaloid vessels on the vitrad surface of the retina of two species of channichthyid fishes (–Hb). (A) *Chaenocephalus aceratus*; (B) *Champsocephalus gunnari*. The cornea, iris, lens and vitreous body were removed to allow viewing of the hyaloid vasculature. The arteries arise from 4–5 main branches and form an extensive series of parallel anastomosing channels. Blood vessels were filled with yellow Microfil™. Scale bars, 3 mm.

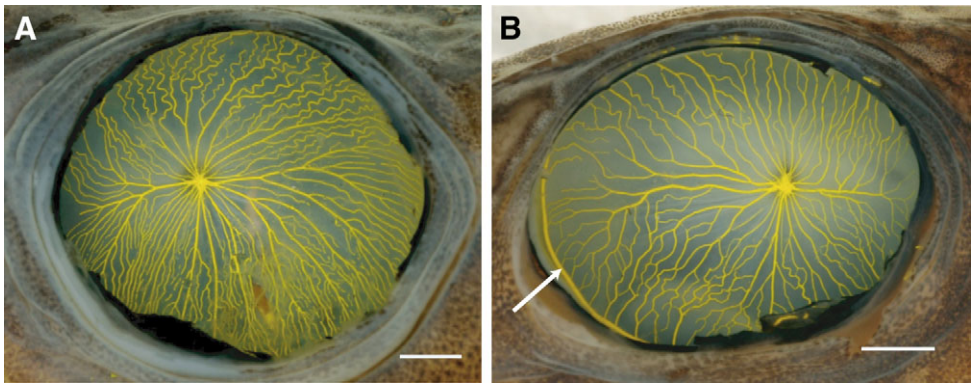

Fig. 3. Representative digital images of the hyaloid vessels on the vitrad surface of the retina of two species of bathydraconid fishes (+Hb). (A) *Gymnodraco acuticeps*; (B) *Parachaenichthyes charcoti*. The cornea, iris, lens and vitreous body were removed to allow viewing of the hyaloid vasculature, here exemplifying a dense and an intermediate radial pattern, respectively. Hyaloid arteries are seen draining to the annular vein (indicated by arrow) in B. Blood vessels were filled with yellow Microfil^{TM}. Scale bars, 3 mm (A); 2 mm (B).

+Hb species (blue symbols, Fig. 5A). The icefish species were not incorporated in our regression analysis because of this marked difference in blood flow from red-blooded species. Examination of the relationship between Hct and IVD further illustrates the validity of this decision.

An equally compelling correlation, in this case positive, exists between Hct and IVD among the red-blooded notothenioids (red symbols in Fig. 5B). As the oxygen delivery capacity per unit volume of blood increases, hyaloid arteries are spaced farther apart. Here, once again, the hemoglobinless icefishes that have the lowest blood oxygen-carrying capacities also show the closest spacing of arteries, but not to the point that would be extrapolated from the relationship among red-blooded species (Fig. 5B). If extrapolated from the relationship between Hct and IVD among red-blooded notothenioids, IVD for icefishes that are completely devoid of Hb would approach 0 mm, i.e. a complete vascular blanket of the visual surface. As with VDI above, the magnitude of anatomical compensation required in IVD is apparently diminished by marked greater perfusion of tissue in the –Hb icefishes.

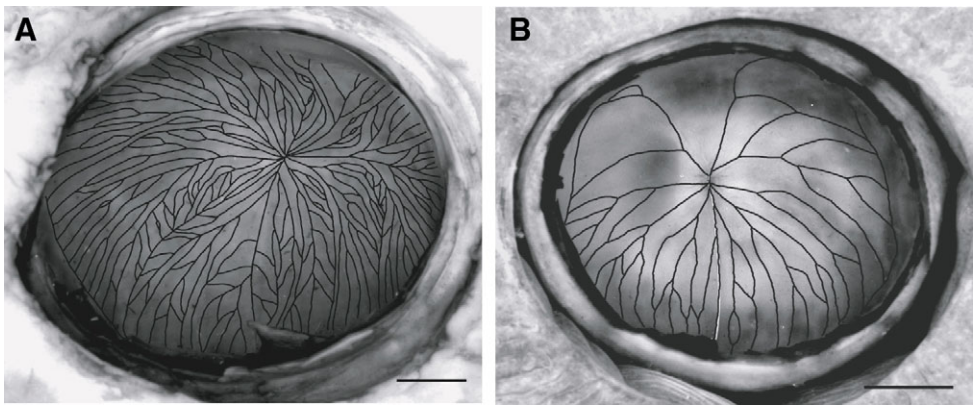

Fig. 4. Representative digital images of the hyaloid vessels on the vitrad surface of the retina of two species of nototheniid fishes (+Hb). (A) *Trematomus hansoni*; (B) *Notothenia coriiceps*. The cornea, iris, lens and vitreous body were removed to allow viewing of the hyaloid vasculature, here exemplifying an intermediate and a sparse radial pattern, respectively. Blood vessels were traced using a digitizing tablet. Scale bars, 3 mm.

Discussion

Retinal tissue is highly aerobic in metabolic poise and requires large amounts of oxygen to sustain normal physiological function (Waser and Heisler, 2004). Because of this aerobic character, maintenance of adequate oxygen tensions is likely to be an acute challenge in eyes of many Antarctic notothenioid fishes, particularly for species of this group in which hemoglobin is expressed at low levels or is completely absent. Previous reports have indicated that dramatic differences exist in geometries of ocular blood vessels when comparing hemoglobinless and red-blooded Antarctic fishes (Eastman, 1988; Eastman and Lannoo, 2004). Those studies qualitatively described substantially higher vascular densities on the vitrad surface of the retina in –Hb species than in +Hb notothenioids but, with the exception of measuring vessel diameters, did not quantify any other morphometric parameter of retinal vascular anatomy. Our measurements provide a more thorough quantitative description of morphometries in retinal vasculatures of several notothenioid fishes, corroborating and extending the earlier qualitative accounts.

To quantify vascular parameters in eyes of notothenioid fishes, we initially either filled the vasculature with a silicone rubber compound or used a gross staining technique and then subsequently employed digital image analysis. In recent years, digital methods have increasingly been employed to quantify biological structures (Abrams et al., 1994; Rieder et al., 1995). Automated image analysis decreases processing time and yields highly reproducible results. The software macro that we developed for the present study resulted in intra-observer variation of <1%, a substantial improvement over previous

Table 2. *Morphometric measurements of vascular anatomies in retinal tissues of Antarctic notothenioid fishes*

	Channichthyidae		Bathydraconidae		Nototheniidae	
	C. aceratus (–Hb)	*C. gunnari* (–Hb)	*G. acuticeps* (+Hb)	*P. charcoti* (+Hb)	*T. hansoni* (+Hb)	*N. coriiceps* (+Hb)
Length density (mm mm^{-2})	5.509±0.317^{a}	5.146±0.497^{a,b}	5.202±0.465^{a,b}	4.400±0.296^{a,b}	3.942±0.080^{b}	2.483±0.214^{c}
Vessel diameter (mm)	0.196±0.009^{a}	0.186±0.002^{a}	0.138±0.003^{b}	0.115±0.004^{c}	ND	ND
Fractional image area (%)	49.13±0.98^{a}	43.75±2.56^{b}	32.97±2.39^{c}	23.79±2.13^{d}	ND	ND
IVD (mm)	0.293±0.016^{a}	0.308±0.030^{a}	0.307±0.030^{a}	0.364±0.027^{a}	0.399±0.008^{a}	0.646±0.051^{b}
VDI (number of intersections/ unit length)	3.507±0.202^{a}	3.276±0.316^{a,b}	3.312±0.296^{a,b}	2.801±0.188^{a,b}	2.491±0.061^{b}	1.581±0.136^{c}

Length density is the length of vessels occupying a given area; Vessel diameter is the width of blood vessels measured to the outside walls; VDI, vascular density index; IVD, intervessel distance; Fractional image area is the percentage of reference area occupied by blood vessels.

Values are means ± s.e.m.; N=5 for *C. aceratus* and *P. charcoti*; N=2 for *C. gunnari*; N=3 for *G. acuticeps* and *T. hansoni;* N=4 for *N. coriiceps*.

Vessel diameter measurements; N=4 for *C. aceratus* and *P. charcoti.*

ND, not determined for technical reasons (see text).

Different superscript letters denote significant differences between species ($P \leqslant 0.05$).

measurement variability with automated systems (Maas et al., 1999; Voss et al., 1984). Results of our analyses demonstrate that the extent of retinal vascular proliferation is directly related to the amount of Hb-containing erythrocytes in the circulation.

Hemoglobinless icefishes display the most elaborate retinal vasculature

C. aceratus and *C. gunnari*, –Hb icefishes, display a distinctive vascular branching pattern with 4–5 large hyaloid arteries originating at the optic disc and anastomosing into closely spaced parallel vessels. This pattern ultimately results in the highest density of blood vessels among all the notothenioids examined. In bathydraconid species (modest Hct levels), the pattern shifts to a more radial distribution, with 4–5 main arteries originating at the optic disc and branching dichotomously; vascular densities also are lower (see below). The species with the highest red cell content examined, *N. coriiceps*, displays a clear radial distribution of very widely separated arteries.

Antarctic notothenioids display a more extensive and homogeneous pattern of hyaloid arteries compared to the majority of teleosts studied to date (Anctil, 1968; Eastman, 1988; Hanyu, 1962). Eastman (Eastman, 1988) described the notothenioid hyaloid pattern as being radially asymmetrical, with slightly greater densities on the ventral and nasal fields. He observed no marked differences in vessel distribution between central and peripheral regions of the retina. This is unlike the unusual pattern seen in the surface-living cyprinodontid, *Fundulus grandis*, where a highly vascularized area centralis is observed ventral to the optic disc (Copeland, 1976). Vascular geometries of notothenioids that we examined generally conform to the above characterization by Eastman, with greater densities on the ventral aspect of the retina (data not shown).

Mass-specific blood volumes of –Hb icefishes are in the range of 7–9% of body mass, or approximately two- to fourfold greater than those characteristic of most red-blooded fishes (Kock, 2005). Some, but not all, of this additional volume might be accounted for by the significantly larger bore of blood vessels in icefishes than their red-blooded counterparts. But, even this possibility is not valid for all tissues. For example, mean capillary cross-sectional area in skeletal muscle of *C. aceratus* is ~1.6-fold greater than that measured in *N. coriiceps* (O'Brien et al., 2003). Assuming a cylindrical geometry, this would correspond only to an identical 1.6-fold elevation in vascular volume of icefish skeletal muscle compared to the tissue in red-blooded species, if vascular densities were equivalent in both species; but they are not. Both capillary density and capillary length density in pectoral muscle are lower in *C. aceratus* than in *N. coriiceps* (O'Brien et al., 2003) and it has been argued that instantaneous blood volume in the microcirculation of icefish locomotory muscles is similar to that seen in other teleosts (Egginton and Rankin, 1998). So, how can we account for accommodation of a greater organismal volume of blood in the circulation of icefishes than red-blooded species? At least part of the answer appears to be the proliferation of vasculature seen in other tissues of icefishes.

Average length densities of retinal vessels from –Hb channichthyids vary little from mean densities in +Hb bathydraconids that possess intermediate Hcts, but are ~1.5-fold greater than mean length densities observed in +Hb nototheniids characterized by the greatest content of red blood cells. VDI of retinal hyaloid arteries and the corresponding distance separating them in the vascular array show a much more regular progression (Table 2). Icefishes display the greatest vascular densities and smallest intervessel distances, followed by bathydraconid species, while nototheniids with the highest Hcts clearly possess the lowest vascular densities and greatest intervessel distances. Hb-deficient notothenioids thus maintain normal biological function in the eye by compensations that include high densities of large-bore blood vessels and short path lengths for oxygen diffusion.

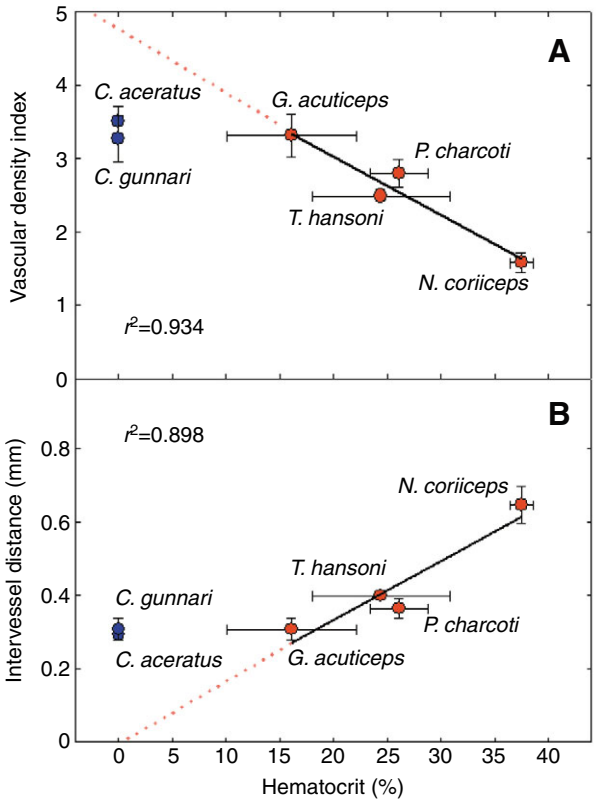

Fig. 5. Hematocrit is related to vascular density index (VDI) and intervessel distance (IVD). (A) Among four red-blooded notothenioids with a >2.3-fold range of Hct, VDI in retinal tissue is inversely correlated with Hct (r^2=0.934). (B) Intervessel distance in retinal tissue, in the same four species, is positively correlated with Hct (r^2=0.898). Values are means ± s.e.m.; N=5 for *C. aceratus* and *P. charcoti*; N=2 for *C. gunnari*; N=3 for *G. acuticeps* and *T. hansoni*; N=4 for *N. coriiceps*. Channichthyids were not included in the regression analysis relating Hct to anatomical vascular characteristics because blood flow in icefishes is many times that of +Hb species. These high blood flows permit adequate oxygenation at lower vascular densities and greater spacing between vessels than would be expected based upon the relationship between Hct and these parameters (broken red lines).

The combination of larger bore and more densely distributed blood vessels in –Hb icefishes also results in considerable increases in vascular blood volume of the retina. For example, blood vessels of icefishes are at least 1.5-fold larger in diameter than those of red-blooded notothenioids and vascular densities of icefishes are up to ~2.2 times greater. Thus, we can anticipate that the instantaneous blood volume of retinal vasculature in icefish species should be approximately fivefold greater than that of their high-Hct +Hb relatives. Any other tissues that show similar differences in vascular proliferation between –Hb and +Hb species likewise will contribute significantly to disparities in organismal blood volume that have been documented between icefishes and closely related red-blooded species.

Red blood cell content of +Hb species is directly related to vascular density

The general pattern of compensation described above is a logical one. Aerobic demand of retinal tissue among the species studied is probably similar, given that all are predominantly visual predators, based upon prey items (Gon and Heemstra, 1990). Two possible compensatory mechanisms (or a combination of both) may ensure uniform delivery of oxygen to retinas of animals with decreasing blood oxygen-carrying capacities. First, elevation in the rate of blood flow through vessels will maximize the driving P_{O_2} gradient across the entire length of the exchange surface. This strategy is most evident in the –Hb icefishes, as indicated by their much greater cardiac outputs than observed in +Hb species. Although available data are limited, the range of mass-specific cardiac outputs among the +Hb species is relatively restricted (Axelsson, 2005). Absolute viscosity of blood containing red blood cells is also greater than that of hemoglobinless species (Wells et al., 1990). Consequently, increasing the rate of flow of blood containing erythrocytes through individual vessels would require significant elevation of vascular pressures and does not appear to be a strategy employed by +Hb species. The second possible mechanism for compensation of oxygen delivery is by anatomical proliferation of the vascular array supplying the tissue, which both increases the overall perfusion of the tissue and reduces the diffusional path length for oxygen. We reasoned that vascular proliferation, therefore, must be the predominant means of compensating for reductions in blood oxygen-carrying capacity among the +Hb species. This prompted us to examine more closely the relationship between red blood cell content and vascular densities among red-blooded notothenioids in this study.

Although we were prepared to find a significant correlation between apparent capacity of blood to carry oxygen and anatomical indices for oxygen delivery to retinal tissue, we were surprised at how tightly linked theses features are among the red-blooded species. Across a >2.3-fold range in Hct, a decrease in erythrocyte content of the blood is met with both a compensatory proportional increase in density of blood vessels supplying the retina and a decrease in spacing between the blood vessels (Fig. 5A,B). In other words, the lower apparent oxygen content of blood, the greater the blood supply and shorter the diffusional distance for oxygen – a result that is somewhat satisfying from an intuitive sense. We might initially expect that extrapolation of these relationships to zero Hct would be predictive of values in the –Hb icefish species; yet, this is not the case. Icefish species consistently show lower vascular densities and wider intervessel distances than would be predicted. Upon further reflection, this is not really surprising, given very marked differences in parameters of blood flow between these groups. As mentioned earlier, one of the hallmark characteristics of channichthyid icefishes is their much greater cardiac output than observed in red-blooded relatives. A greater rate of vascular perfusion evidently diminishes the need for these compensations to provide adequate rates of oxygenation of retinal tissue.

What mechanism drives changes in vascular anatomy?

Our study has now added differences in vascular densities of a highly oxidative tissue to a long list of cardiovascular disparities between –Hb icefishes and their red-blooded relatives that appear to have been driven by differences in oxygen-carrying capacity of their bloods. This cause-and-effect relationship is further supported by the tight linkage between vascular anatomy and erythrocyte content of the blood that we observed among red-blooded notothenioids. Yet, the observations alone tell us nothing about underlying mechanisms that yield the different anatomies. At least two possible scenarios may be envisioned. First, these vascular characters may have come about by the process of natural selection operating upon vascular differences that arose through random mutations within the ancestral populations of modern species. Such an explanation, however, begs the question of how the dramatically altered vascular characters of icefishes could have come about so rapidly in light of the relatively short evolutionary history of this group of fishes [ca. 5 MYA (Near et al., 2003)]. The alternative is that some type of physiological feedback mechanism exists such that conditions arising from changes in the level of erythrocytes containing oxygen-binding proteins affect vascular development.

One of the most potent mechanical affectors of angiogenesis in vertebrate animals is shear stress (Brown and Hudlicka, 2003). This rheological force is proportional to both blood viscosity and velocity of flow and inversely proportional to the radius of the blood vessel. Because hematocrit directly affects viscosity, one might speculate that variance in hematocrits observed among the red-blooded species in this study might lead to differences in shear stress that could correlate with retinal vascular densities. It is impossible to evaluate this conjecture rigorously because measurements of velocity of blood flow through the retinas are unavailable. Our observations, however, appear to be at direct odds with shear stress as a causative factor. Reductions in hematocrit will result in decreased viscosity of blood, thus lowering shear stress and presumably reducing this mechanical angiogenic stimulus. Viscosity of whole blood in the hemoglobinless icefishes (Hct=0) is substantially lower than that of their red-blooded counterparts (Wells et al., 1990; Egginton, 1996). Yet, we observed increases in vascular proliferation with decreases in hematocrit among the red-blooded fishes studied and the highest vascular density was measured in a hemoglobinless icefish. On this basis, it seems reasonable to discount shear stress as a major determinant of vascular densities in retinas of Antarctic fishes. What then, might be the causative agent for vascular proliferation?

We have recently suggested an alternative mechanism involving the ubiquitous bioactive molecule, nitric oxide (NO) (Sidell and O'Brien, 2006). The most widely recognized role of NO is that of a potent vasodilator, but it also is known to mediate a pathway that promotes the growth of capillary networks (angiogenesis) (Conway et al., 2001). NO is produced in vertebrate animal tissues in a reaction catalyzed by a family of three isoforms of the enzyme nitric oxide synthase (NOS). There is wide acceptance that the most quantitatively important catabolic reaction of NO in vertebrate animals is its reaction with oxyferrohemoglobin (oxyHb). Reaction of NO with oxyHb is very rapid and yields products of metHb (methemoglobin) and nitrate; the reaction is considered to be the major route of elimination of NO from the body and the major source of circulating nitrate in vertebrates (Kerwin, Jr et al., 1995). Thus, reductions in levels of circulating Hb should lead to reduction in the rate at which NO is degraded and elevation of its steady-state levels. Elevated NO, in turn, could trigger vascular proliferation. The data we report here are consistent with such an hypothesis.

If the mechanism described above proves to be correct, the implications are provocative. Such a mechanism suggests that notothenioids (like other vertebrates) intrinsically possess physiological feedback systems that may rapidly trigger changes in vascular density in response to altered concentration of circulating Hb. The logical extension of this is that physiology of ancestral channichthyids may have accelerated the evolution of compensations to the mutational loss of Hb expression and the development of their extreme cardiovascular characteristics.

List of abbreviations

Hct	hematocrit
Hb	hemoglobin
–Hb	hemoglobinless channichthyid icefishes
+Hb	red-blooded notothenioid fishes
ROI	region of interest tool
VDI	vascular density index
IVD	intervessel distance
FIA	fractional image area
NO	nitric oxide
NOS	nitric oxide synthase

We gratefully acknowledge the support personnel of Raytheon Polar Services at Palmer Station and aboard the *Laurence M. Gould* and the masters and crew of the ARSV *Laurence M. Gould* for a safe and successful field season in Antarctica. Additional thanks to Dr Seth Tyler for assistance with the histological staining. Funding for this research was provided by US NSF Grants ANT 04-37887 to B.D.S. and ANT 04-36190 to J.T.E.

References

Abrams, D. C., Facer, P., Bishop, A. E. and Polak, J. M. (1994). A computer-assisted stereological quantification program: OpenStereo. *Microsc. Res. Tech.* **29**, 240-247.

Anctil, M. (1968). Intraocular vascular supply in some marine teleosts. *Rev. Can. Biol.* **27**, 347-355.

Axelsson, M. (2005). The circulatory system and its control. In *Fish Physiology, Vol. 22, The Biology of Polar Fishes* (ed. A. P. Farrel and J. Steffensen), pp. 239-280. San Diego: Elsevier Academic Press.

Brown, M. D. and Hudlika, O. (2003). Modulation of physiological angiogenesis in skeletal muscle by mechanical forces: involvement of VEGF and metalloproteinases. *Angiogenesis* **6**, 1-14.

Chase, J. (1982). The evolution of retinal vascularization in mammals. A

comparison of vascular and avascular retinae. *Ophthalmology* **89**, 1518-1525.

Conway, E. M., Collen, D. and Carmeliet, P. (2001). Molecular mechanisms of blood vessel growth. *Cardiovasc. Res.* **49**, 507-521.

Copeland, D. E. (1976). The anatomy and fine structure of the eye in teleost. IV. The choriocapillaris and the dual vascularization of the area centralis in *Fundulus grandis*. *Exp. Eye Res.* **22**, 169-179.

Copeland, D. E. (1980). Functional vascularization of the teleost eye. *Curr. Top. Eye Res.* **3**, 219-280.

Eastman, J. T. (1988). Ocular morphology in Antarctic notothenioid fishes. *J. Morphol.* **196**, 283-306.

Eastman, J. T. (1993). *Antarctic Fish Biology: Evolution in a Unique Environment*. San Diego: Academic Press.

Eastman, J. T. (2005). The nature of the diversity of Antarctic fishes. *Polar Biol.* **28**, 93-107.

Eastman, J. T. and Lannoo, M. J. (2003). Diversification of brain and sense organ morphology in Antarctic dragonfishes (Perciformes: Notothenioidei: Bathydraconidae). *J. Morphol.* **258**, 130-150.

Eastman, J. T. and Lannoo, M. J. (2004). Brain and sense organ anatomy and histology in hemoglobinless Antarctic icefishes (Perciformes: Notothenioidei: Channichthyidae). *J. Morphol.* **260**, 117-140.

Eastman, J. T. and Lannoo, M. J. (in press). Brain and sense organ anatomy and histology of two species of phyletically basal non-Antarctic thornfishes of the Antarctic suborder Notothenioidei (Perciformes: Bovichtidae). *J. Morphol.* **268**.

Egginton, S. (1996). Blood rheology of Antarctic fishes: viscosity adaptations at very low temperatures. *J. Fish Biol.* **48**, 513-521.

Egginton, S. and Rankin, C. (1998). Vascular adaptations for a low pressure/high flow blood supply to locomotory muscles of Antarctic icefish. In *Fishes of Antarctica: A Biological Overview* (ed. G. di Prisco, E. Pisano and A. Clarke), pp. 185-195. Milan: Springer-Verlag.

Fitch, N. A., Johnston, I. A. and Wood, R. E. (1984). Skeletal muscle capillary supply in a fish that lacks respiratory pigments. *Respir. Physiol.* **57**, 201-211.

Gon, O. and Heemstra, P. C. (ed.) (1990). *Fishes of the Southern Ocean*. Grahamstown: J. L. B. Smith Institute of Ichthyology.

Hanyu, I. (1962). Intraocular vascularization in some fishes. *Can. J. Zool.* **40**, 87-106.

Hemmingsen, E. A. (1991). Respiratory and cardiovascular adaptations in hemoglobin-free fish: resolved and unresolved problems. In *Biology of Antarctic Fish* (ed. G. di Prisco, B. Maresca and B. Tota), pp. 191-203. New York: Springer-Verlag.

Hemmingsen, E. A. and Douglas, E. L. (1970). Respiratory characteristics of the hemoglobin-free fish *Chaenocephalus aceratus*. *Comp. Biochem. Physiol.* **33**, 733-744.

Hemmingsen, E. A., Douglas, E. L., Johansen, K. and Millard, R. W. (1972). Aortic blood flow and cardiac output in the hemoglobin-free fish *Chaenocephalus aceratus*. *Comp. Biochem. Physiol.* **43A**, 1045-1051.

Holeton, G. F. (1970). Oxygen uptake and circulation by a hemoglobinless Antarctic fish (*Chaenocephalus aceratus* Lonnberg) compared with three red-blooded Antarctic fish. *Comp. Biochem. Physiol.* **34**, 457-471.

Kawall, H. G., Torres, J. J., Sidell, B. D. and Somero, G. N. (2002). Metabolic cold adaptation in Antarctic fishes: evidence from enzymatic activities of brain. *Mar. Biol.* **140**, 279-286.

Kerwin, J. F., Jr, Lancaster, J. R., Jr and Feldman, P. L. (1995). Nitric oxide: a new paradigm for second messengers. *J. Med. Chem.* **38**, 4343-4362.

Knox, G. A. (1970). Antarctic marine ecosystems. In *Antarctic Ecology*. Vol. 1 (ed. M. W. Holdgate), pp. 69-96. London: Academic Press.

Kock, K.-H. (2005). Antarctic icefishes (Channichthyidae): a unique family of fishes. A review, Part I. *Polar Biol.* **28**, 862-895.

Laws, R. M. (1985). The ecology of the Southern Ocean. *Am. Sci.* **73**, 26-40.

Lewis, R. W. and Perkin, R. G. (1985). The winter oceanography of McMurdo Sound, Antarctica. In *Antarctic Research Series, Vol. 43, Oceanology of the Antarctic Continental Shelf* (ed. S. S. Jacobs), pp. 145-165. Washington: American Geophysical Union.

Littlepage, J. L. (1965). Oceanographic investigations in McMurdo Sound, Antarctica. In *Antarctic Research Series, Vol. 5, Biology of the Antarctic Seas II* (ed. G. A. Llano), pp. 1-37. Washington: American Geophysical Union.

Maas, J. W. M., Le Noble, F. A. C., Dunselman, G. A. J., de Goeij, A. F. P. M., Struyker Boudier, H. A. J. and Evers, J. L. H. (1999). The chick embryo chorioallantoic membrane as a model to investigate the angiogenic properties of human endometrium. *Gynecol. Obstet. Invest.* **48**, 108-112.

Near, T. J., Pesavento, J. J. and Cheng, C.-H. (2003). Mitochondrial DNA, morphology and the phylogenetic relationships of Antarctic icefishes (Notothenioidei: Channichthyidae). *Mol. Phylogenet. Evol.* **28**, 87-98.

Nicol, J. A. C. (1989). *The Eyes of Fishes*. Oxford: Oxford University Press.

O'Brien, K. M., Skilbeck, C., Sidell, B. D. and Egginton, S. (2003). Muscle fine structure may maintain the function of oxidative fibres in haemoglobinless Antarctic fishes. *J. Exp. Biol.* **206**, 411-421.

Rieder, M. J., O'Drobinak, D. M. and Greene, A. S. (1995). A computerized method for determination of microvascular density. *Microvasc. Res.* **49**, 180-189.

Ruud, J. T. (1954). Vertebrates without erythrocytes and blood pigment. *Nature* **173**, 848-850.

Sidell, B. D. and O'Brien, K. M. (2006). When bad things happen to good fish: the loss of hemoglobin and myoglobin expression in Antarctic icefishes. *J. Exp. Biol.* **209**, 1791-1802.

Strick, D. M., Waycaster, R. L., Montani, J. P., Gay, W. J. and Adair, T. H. (1991). Morphometric measurements of chorioallantoic membrane vascularity: effects of hypoxia and hyperoxia. *Am. J. Physiol.* **260**, H1385-H1389.

Voss, K., Jacob, W. and Roth, K. (1984). A new image analysis method for the quantification of neovascularization. *Exp. Pathol.* **26**, 155-161.

Walls, G. L. (1942). *The Vertebrate Eye and its Adaptive Radiation, Bulletin No. 19*. Bloomfield Hills, MI: Cranbrook Institute of Science.

Waser, W. P. and Heisler, N. (2004). Oxygen delivery to the fish eye: blood flow in the pseudobranchial artery of rainbow trout (*Oncorhynchus mykiss*). *Fish Physiol. Biochem.* **30**, 77-85.

Weibel, E. R. (1979). *Stereological Methods: Practical Methods for Biological Morphometry.* Vol. 1. New York: Academic Press.

Wells, R. M. G., Ashby, M. D., Duncan, S. J. and Macdonald, J. A. (1980). Comparative study of the erythrocytes and haemoglobins in nototheniid fishes from Antarctica. *J. Fish Biol.* **17**, 517-527.

Wells, R. M. G., Macdonald, J. A. and di Prisco, G. (1990). Thin-blooded Antarctic fishes: a rheological comparison of the haemoglobin-free icefishes *Chionodraco kathleenae* and *Cryodraco antarcticus* with a red-blooded nototheniid, *Pagothenia bernacchii*. *J. Fish Biol.* **36**, 595-609.